Optik 153 (2018) 109–116

Contents lists available at ScienceDirect

Optik

journal homepage: www.elsevier.de/ijleo

Full length article

Thermoluminescence of $LaAlO_3$:C crystals grown by different mixing methodologies applied to UV dosimetry

Neriene Alves [a], Ahmed Kadari [b,*], Wilmar Barbosa Ferraz [c], Luiz Oliveira de Faria [a,c]

[a] Departamento de Engenharia Nuclear, Universidade Federal do Estado de Minas Gerais, Av. Antônio Carlos, 6627, CEP. 31270-901 Belo Horizonte, MG, Brazil
[b] Department of Chemistry, Faculty of Sciences of the Matter, Ibn Khaldoun University of Tiaret, BP P 78 Zaaroura, Tiaret, Algeria
[c] Centro de Desenvolvimento da Tecnologia Nuclear, Av. Antonio Carlos 6627, C.P. 941, 30161-970 Belo Horizonte, MG, Brazil

ARTICLE INFO

Article history:
Received 28 June 2017
Accepted 3 October 2017

Keywords:
TL
$LaAlO_3$
UV dosimeter
Dose response
Trapping parameters

ABSTRACT

In this paper, thermoluminescence (TL) properties such as glow curves analysis, dose response linearity and some dosimetric characteristics of pure and carbon doped lanthanum aluminate ($LaAlO_3$) produced by different syntheses using the solid state reaction method are investigated, after exposure to different UV radiation doses. The effect of different syntheses on the TL glow curves structures is also investigated and discussed. TL glow-curve deconvolution (CGD) methods and the Chen's peak shape methods were used to analyze the sets of TL glow curves. The kinetic parameters of TL single peaks were computed. Additionally, the life times (τ) of electrons in trap for all samples were determined and calculated. A good linear dose response over the dose range from 0.21 to 1.26 mJ/cm^2 has been attributed to both samples (B and C).

1. Introduction

Thermoluminescence (TL) is the process of light emission from a semiconductor or insulator when it is heated after the previous absorption of energy from ionizing radiation [1]. Many natural and synthetic materials exhibit this phenomenon [2,3]. Application of this phenomenon is found in several disciplines like dosimetry [4], archaeology [5] and solid state research as a tool to investigate defects in some luminescent materials [1,5].

Due to their excellent chemical and thermal stability; lanthanum aluminate ($LaAlO_3$) polycristals have been widely used as a substrate of high-temperature superconductor [6–9]. TL properties of lanthanum aluminate ($LaAlO_3$) applied to ultraviolet radiation dosimetry has been previously studied [10–12]. UV radiation can induce certain deleterious effects, such as erythema, painful inflammation of the membrane of the eye and skin cancer [13,14]. Therefore, there is a push for new and high-performance radiometers, for direct dose evaluation, and also TL-based dosimeters for post-exposure dose evaluation. ZrO_2 + PTFE (TL dosimeter) and a-Al_2O_3:C (PTTL dosimeter) are among the best TL materials ever discovered for UV dosimetry, presenting minimum detection values of 0.002 mJ/cm^2 and 0.050 mJ/cm^2, respectively [15,16]. Recently, Lanthanum aluminate ($LaAlO_3$) single crystals grown by hydrothermal condition and co-doped with trivalent Ce^{3+} and Dy^{3+} rare earth ions have been reported to show high thermoluminescent response after exposure to low doses of ultraviolet

* Corresponding author.
E-mail addresses: kadariahmed_14@yahoo.fr, ahmed.kadari27@gmail.com (A. Kadari).

https://doi.org/10.1016/j.ijleo.2017.10.018
0030-4026/

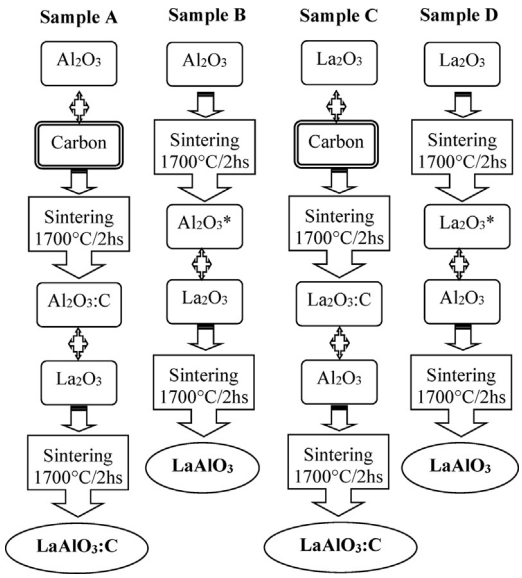

Fig. 1. Schematic diagrams illustrating the synthesis pathways used to produce pure and carbon doped $LaAlO_3$:C samples.

Table 1
Samples denomination and syntheses methodologies.

Sample denomination	Mixing Methodology	Resulting crystal
A	Al_2O_3:C + La_2O_3	$LaAlO_3$:C
B.	Al_2O_3 + La_2O_3	$LaAlO_3$
C	La_2O_3:C + Al_2O_3	$LaAlO_3$:C
D	La_2O_3 + Al_2O_3	$LaAlO_3$

radiation [10]. On the other hand, alpha-Al_2O_3:C crystals have been reported to shown excellent TL properties for both gamma and UV fields (Akselrod et al., [17]), Thus, in a previous work, we investigated the possibility of doping $LaAlO_3$ crystals with carbon atoms, aiming the enhancing of its TL properties for UV and also for gamma fields [12]. We have sintered equimolar amounts of alpha-Al_2O_3, La_2O_3 and carbon atoms by the solid state method, in order to obtain polycrystalline $LaAlO_3$:C powder. The material showed very high TL output and linear response for UV spectral irradiance ranging from 0.04 to 1.20 $mJcm^{-2}$.

In the present paper, we explored four different mixing methodologies to produce pure and carbon doped $LaAlO_3$ crystals by the solid state reaction method. Particularly, we are interested in producing $LaAlO_3$:C crystals by two different ways: in the first route Al_2O_3 powder plus carbon atoms will be sintered together at high temperature and then mixed with La_2O_3 powder. In a second route La_2O_3:C powder will be sintered at high temperature and then mixed with Al_2O_3 powder.

The aim of this work is to find what sintering route produces the better TL responses for undoped and carbon doped $LaAlO_3$ crystals, after exposure to UV fields. On the other hand, in order to improve the understanding of the whole of carbon atoms in the TL process, detailed kinetics study of trapping parameters of TL glow peaks is also reported.

2. Experimental procedure

Lanthanum aluminate polycristals ($LaAlO_3$) were synthesized by solid state reaction method by mixing equimolar ratios of Al_2O_3 (Vetec, 99.99%) and La_2O_3 (Alfa, 99.98%). The mixed powder was weighed and then manually grinded in agate mortar with 0.1 wt.% of carbon atoms. In order to investigate the influence of the mixing methodology on the TL output of carbon doped $LaAlO_3$ crystals, samples were produced using four different combinations of aluminum oxide (Al_2O_3), lanthanum oxide (La_2O_3) and carbon (C) atoms on the synthesis process. At the end of the synthesis stage all samples were annealed at 950 °C for 30 min, for thermally emptying the electron traps (to remove captured charge carriers from trap centers). The schematic diagrams illustrating the syntheses stages are shown in Fig. 1.

The samples obtained by different mixing methodology depicted on the above diagrams were denominated according to Table 1.

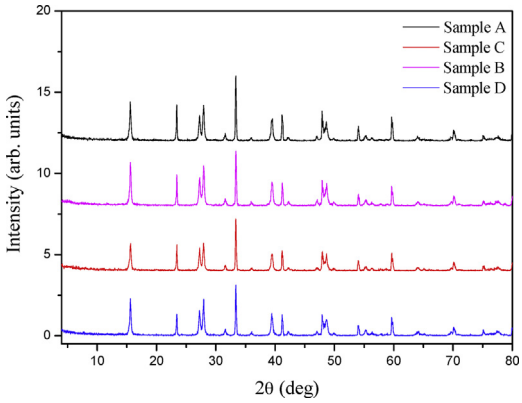

Fig. 2. XRD patterns of all samples produced by four different syntheses.

Table 2
FWHM and particle size values pure and carbon doped $LaAlO_3$ samples obtained from the XRD patterns.

Sample	2θ (deg)	FWHM (deg)	D (Å)
A	33.38	0.18	467.18
B	33.39	0.18	467.18
C	33.38	0.16	517.24
D	33.39	0.16	517.24

2.1. Measurements

In order to confirm the formation of $LaAlO_3$ phase, all samples were analyzed using Regaku D/Max ÚLTIMA X-ray diffractometer with CuKα radiation (λ = 1.54 Å) for 2 theta ranging from 4° to 80°. The scanning rate was set to 0.02°/s. The UV irradiation was performed using a commercial 8WUV fluorescent lamp. The spectral irradiance at the lamp surface was 2.98 mJ/cm^2, measured using a calibrated radiometer UVX100 E-22476 with a 254 nm sensor. Thermoluminescent measurements were performed using the RISO TL/OSL DA20TL reader, with a heating rate of 10 °C/s. The TL signal was integrated from 100 °C up to 300 °C.

3. Results and discussions

3.1. X ray diffraction (XRD)

The crystalline structure of all studied samples was checked by XRD technique. The X-ray diffraction patterns of samples produced by the four different mixing methodologies are shown in Fig. 2. All samples investigated are in the rhombohedral crystallographic phase of $LaAlO_3$, in agreement with the JCPDS 31-0022 card. However, peaks assigned to lanthanum hydroxide phase (JCPDS 36–1481) have also been identified. The amount of $LaAlO_3$ and $La(OH)_3$ were in the range of 35–43% of and 57–65%, respectively. This was considered an unexpected result once stoichiometric amounts of lanthanum oxide and aluminum oxide were used to the reaction. Except for $LaAlO_3$ and $La(OH)_3$, there were no peak shifting or the presence of a second phase for samples produced by the four different syntheses.

The width of the XRD peak increases as the size of the particle (D) decreases. The size of the crystallites has been estimated from the full width at half maximum (FWHM) of the most intense peak. The crystallite dimension (D) was calculated using the well-known Scherer's equation [18]:

$$D = \frac{0.9.\lambda}{\beta.\cos\ \theta},$$

where D is the particle size, β is the FWHM, λ is the wavelength of X ray source; θ is the angle of diffraction. Table 2 shows the values of the FWHM and the particle size obtained from the diffraction patterns given in Fig. 2. It is seen that the crystallite dimensions from samples C and D are equal (517. 24 Å) and larger than crystallites from samples A and B (467.18 Å). Thus, it seems that the methodology where the carbon doped La_2O_3:C and undoped La_2O_3 powders are first sintered at high temperature, produces larger crystallites.

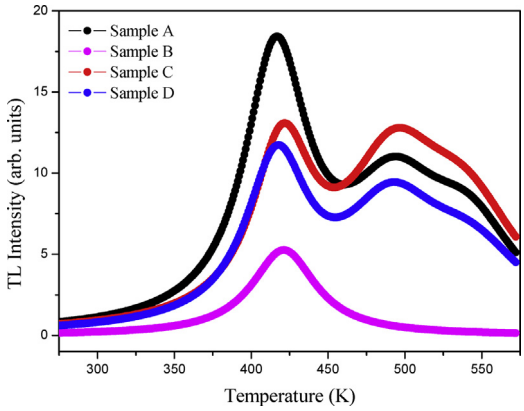

Fig. 3. TL glow curves of pure and carbon doped $LaAlO_3$ crystals produced by four different syntheses.

3.2. Thermoluminescence properties

Thermoluminescence (TL) glow curves of pure and (0.1 wt.%) carbon doped mixture of $LaAlO_3$ and $La(OH)_3$, produced by four different mixing methodologies are shown in Fig. 3. These crystals were irradiated with UV lamp at the range from 0.042 to 1.26 mJ/cm^2. The main TL glow peak for all samples was located at 415 K, which was characterized as the principal dosimetric trap in these crystals; two peaks have also been observed at 493 K and 548 K for samples A, C and D. These peaks were reported in previously published works [11,12]. Sample B presents only one strong peak located at 415 K. It can be seen in both samples A and C that, with the presence of carbon atoms in these crystals lattices, the TL output were bigger than undoped samples. However, a very small shift was found in the glow peak location. It could be noted that all thermoluminescence glow curves of these crystal depends on many factors such as the synthesis pathways, the kind of impurities and the heating rate. It is clear in this study that carbon atoms are the key factor that influences the thermoluminescence properties on the mixture.

It can be noted that carbon atoms in these materials play the role of a dopant and also that four-valent carbon anions replace the two-valent anions of oxygen during the crystal growth process [18]. It has been showed that carbon (C) at the oxygen (O) site acts as a charge compensator to stabilize the F^+ center, thereby enhancing the TL signal at 465 K. Also, carbon (C) at aluminum (Al) site can serve as electron traps for thermoluminescence emission process in α-Al_2O_3 [19].

Lanthanum oxide is highly hygroscopic and rapidly converts to lanthanum hydroxide ($La(OH)_3$) when at moist atmosphere, as observed by Neumann, et al., and Fleming et al. They conclud that after 24 h La_2O_3 is totaly converted to $La(OH)_3$ [20,21]. The thermoluminescence properties of lanthanum oxide was studyed by Soliman et al. [22]. They evaluated the sensitivity of thermoluminescence detectors based on commercial lanthanum oxide (La_2O_3) for beta, gamma, and UV radiation. La_2O_3 is considered a promising phosphor for the detection of UV fields and is sugested to application in ultraviolet dosimetry. According to Fleming et al., it is probable that the lantanum oxide used by Soliman is actually a lanthanum hidroxide. In this context, the TL curves shown in this paper represent a sum of individual $LaAlO_3$ and $La(OH)_3$ TL peaks. However, they have resulted in a material more sensitive than La_2O_3 and $LaAlO_3$ already reported in the literature [11,12,22].

3.2.1. TL glow curve analysis

The thermoluminescent glow curves analysis was performed by the TL glow-curve deconvolution functions for first, second and general orders of kinetics, i.e. the GCD technique that has been applied widely since the 80s. [23]. It is shown in Fig. 4 the deconvolution of TL glow curves for pure and carbon doped $LaAlO_3$ crystals. It can be seen from these results that all experimental curves are composed by four singles peaks, except the sample B which is composed by three peaks. The thermoluminescence glow peak is related to the trap levels that exist in the band gap of a semiconductor or insulator material. These energies levels are characterized by a set of kinetic parameters such as: activation energy (E), order of kinetics (b) and frequency factor (s). In our study, these parameters are calculated by using the Chen's peak shape method [1]. The calculated kinetics parameters are listed in Table 3. The RT lifetimes (τ) of electron in traps can be evaluated by the following formula,

$$\tau = \frac{1}{s} \exp\left(\frac{E}{k_B T}\right),$$

where s is the frequency factor and k_B is the Boltzmann constant. The RT lifetimes of traps values are reported in Table 3.

Thermoluminescence sensitivity of pure and carbon doped $LaAlO_3$ crystals depend strongly on the exposure time. Fig. 5 shows the maximum TL intensity response of samples B and C as a function of the exposure time; selected points in these curves correspond to a period of 1, 5, 15 and 30 s.

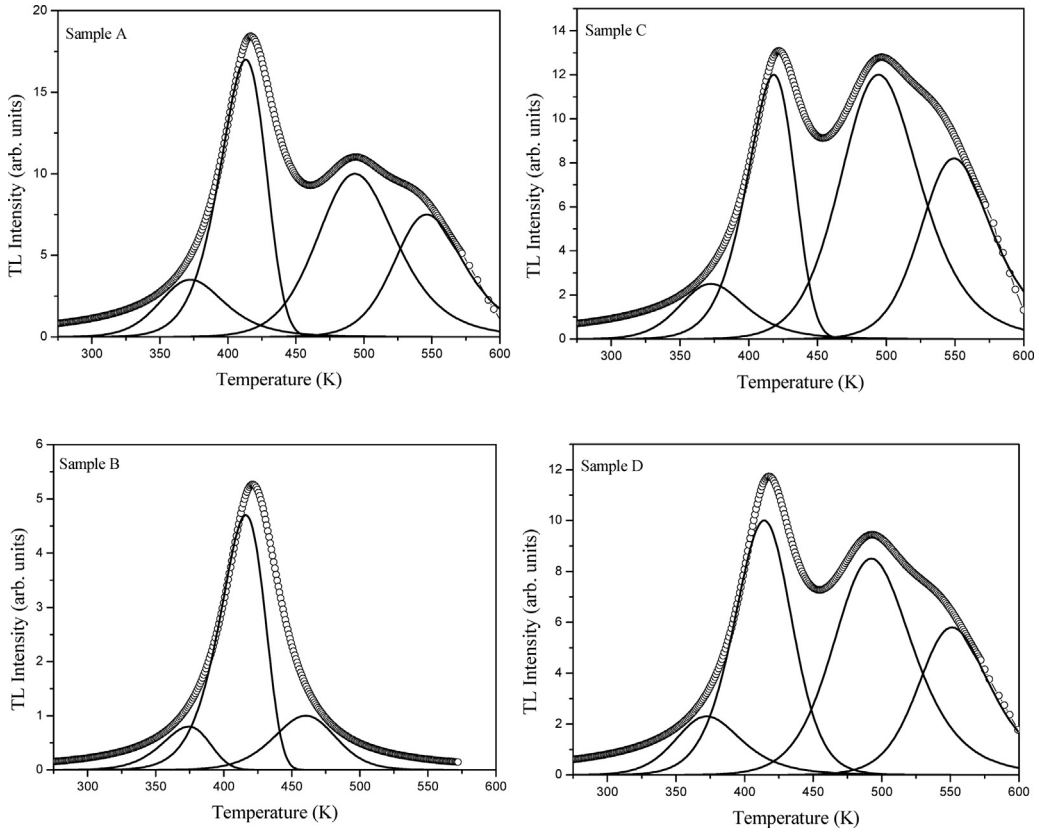

Fig. 4. Deconvolution of thermoluminescence glow curves for pure and carbon doped $LaAlO_3$ crystals.

Table 3
Kinetic parameters values of TL peaks determined by the Chen's peak shape method.

Samples	Peak n°	T_{max} (K)	μ_g	b	β (°C/s)	E_ω (eV)	E_τ (eV)	E_δ (eV)	E_{avr} (eV)	s (s^{-1})	τ at 293 K (s)
A.	1	372.43	0.53	2.00	10	0.702	0.693	0.708	0.701	1.65×10^9	6.92×10^2
	2	413.57	0.42	1.01		0.872	0.859	0.878	0.869	2.35×10^{10}	3.77×10^4
	3	493.28	0.52	1.99		1.012	1.016	1.010	1.010	9.33×10^9	2.53×10^7
	4	546.43	0.53	2.00		1.447	1.469	1.421	1.446	1.14×10^{13}	6.54×10^{11}
B	1	374.14	0.44	1.13	10	0.725	0.705	0.742	0.724	3.40×10^9	8.36×10^2
	2	416.14	0.42	0.99		0.990	0.901	0.890	0.898	4.52×10^{10}	6.18×10^4
	3	459.85	0.49	1.58		1.012	0.989	1.027	1.009	6.15×10^{10}	3.69×10^6
C	1	372.43	0.53	2.00	10	0.702	0.693	0.708	0.701	1.65×10^9	6.92×10^2
	2	417.85	0.44	1.15		0.936	0.916	0.948	0.933	1.12×10^{11}	9.99×10^4
	3	494.14	0.53	2.00		1.018	1.010	1.021	1.016	1.03×10^{10}	2.91×10^7
	4	549.00	0.54	2.00		1.475	1.508	1.440	1.474	1.82×10^{13}	1.24×10^{12}
D	1	372.43	0.53	2.00	10	0.702	0.693	0.708	0.701	1.65×10^9	6.92×10^2
	2	414.43	0.48	1.44		0.856	0.831	0.875	0.854	1.36×10^{10}	3.60×10^4
	3	492.43	0.52	1.96		1.006	0.993	1.012	1.004	8.39×10^9	2.22×10^7
	4	551.57	0.53	2.00		1.439	1.457	1.416	1.437	7.00×10^{12}	4.46×10^{11}

3.2.2. *Linearity curves*

Thermoluminescence response of any TL material is directly related to the amount of absorbed radiation dose. A material is said to be good TL dosimeter when its response to absorbed dose is linear over a wide dose range. TL glow curve of UV irradiated pure and carbon doped $LaAlO_3$ crystals with different doses is shown in Fig. 6. To study the linearity, all samples were irradiated with the same UV doses ranging from 0.042 to 1.26 mJ/cm^2. As it can be seen, the shapes of the glow curves in these figures remained unchanged regardless of the increased dose.

The TL output intensities shown in Fig. 6, for pure and carbon doped $LaAlO_3$ crystals are plotted as a function of UV irradiance in Fig. 7. The result showed that there was a good linear dose response over the dose range from 0.21 to 1.26 mJ/cm^2, for both samples B and C. The TL response of these two samples is shown in Fig. 8. The linear fitting provided correlation coefficients equal to 0.9827 and 0.9999 for samples B and C, respectively. We then conclude that the best TL response for

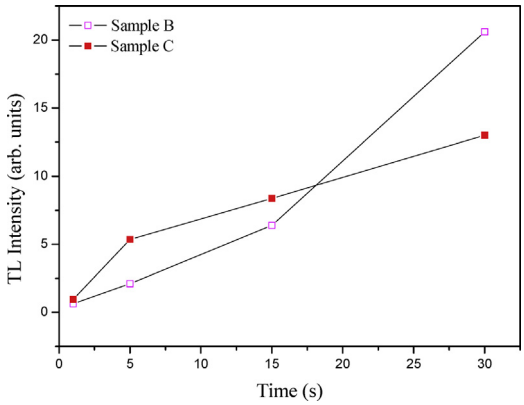

Fig. 5. Maximum TL response of samples B and C as a function of the exposure time.

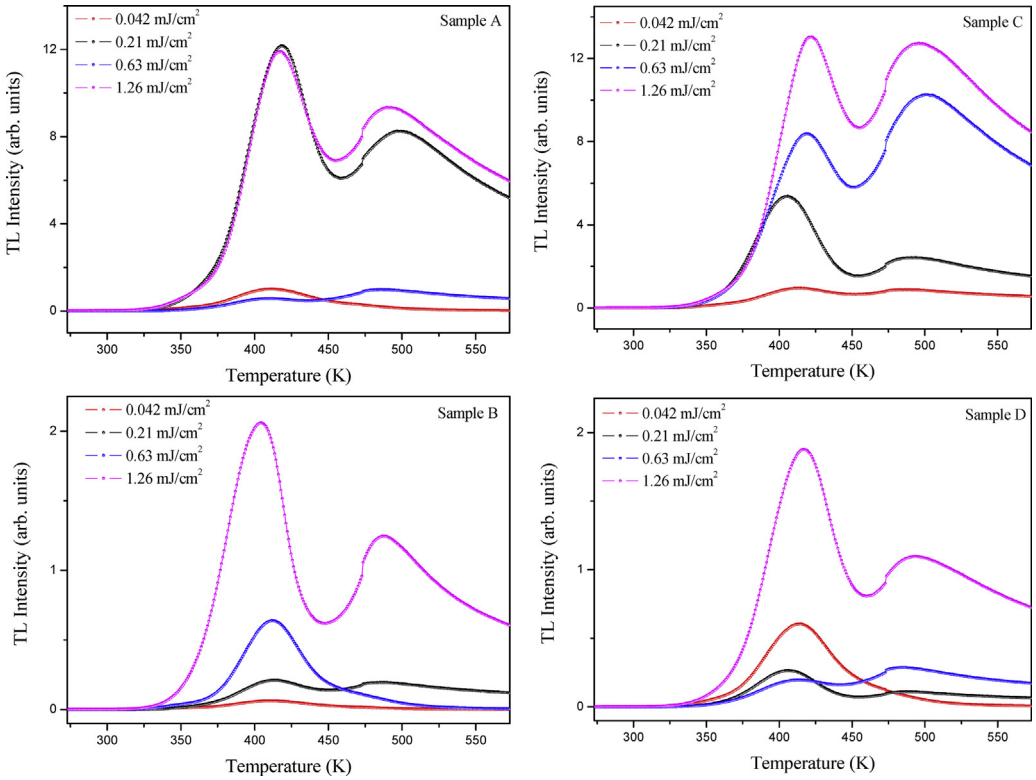

Fig. 6. TL glow curve of pure and carbon doped $LaAlO_3$ crystals at different dose of UV exposure.

UV fields was found to sample C, which was grown by first sintering La_2O_3 together carbon atoms and then sintering again the resulting La_2O_3:C together Al_2O_3.

4. Conclusion

In this paper, thermoluminescence and dosimetric characteristics of pure and carbon doped lanthanum aluminate ($LaAlO_3$) crystals irradiated by different UV doses were studied and discussed. All samples studied were produced by solid state reaction method with different mixing methodologies. The sets of trapping parameters, such as; activation energy (E) and frequency factor (s) of all thermoluminescence (TL) glow peaks of samples, were calculated by Chen's peak shape methods. A good linear dose response over the UV dose range from 0.21 to 1.26 mJ/cm^2 has been attributed to both samples B and C, with correlation coefficients equal to 0.9827 and 0.9999, respectively.

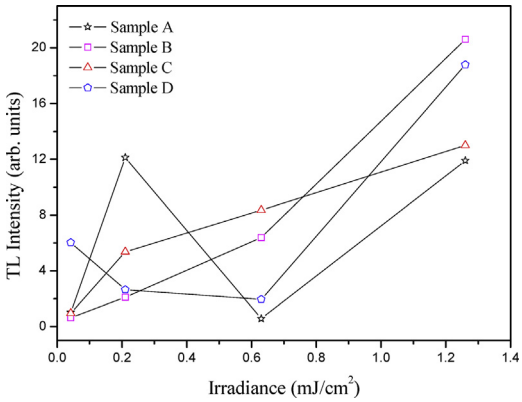

Fig. 7. TL dose response curves of UV doses irradiated pure and carbon doped $LaAlO_3$ crystals.

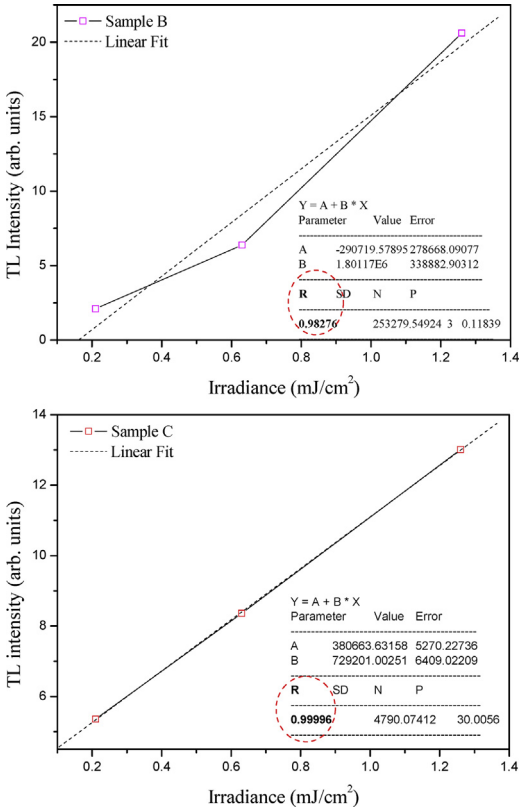

Fig. 8. TL intensity versus UV dose for samples B and C exposed to 0.042, 0.21, 0.63 and 1.26 mJ/cm^2.

Acknowledgments

This work was supported by Conselho Nacional de Desenvolvimento Científico e Tecnológico (CNPq), Coordenação de Aperfeiçoamento de Pessoal de Nível Superior (CAPES), Fundação de Amparo à Pesquisa do Estado de Minas Gerais (FAPEMIG), Comissão Nacional de Energia Nuclear (CNEN).

References

[1] R. Chen, S.W.S. McKeever, Theory of Thermoluminescence and Related Phenomena, World Scientific, Singapore, 1997.
[2] P.P. Pal, J. Manam, Photoluminescence and thermoluminescence studies of Tb^{3+} doped ZnO nanorods, Mater. Sci. Eng.: B 178 (2013) 400–408.
[3] L.E. Alarćon, J.E. Barajas, E. Camps, S. Muhl, E.H. Poniatowski, S. Romero, B. Salinas, Thermoluminescent response of carbon nitride thin films deposited by laser ablation, Mater. Sci. Eng.: B 90 (2002) 79–83.
[4] S.W.S. McKeever, Thermoluminescence of Solids, Cambridge University Press, 1985.

[5] M.J. Aitken, Thermoluminescence Dating, Academic, London, 1985.
[6] J. Kaur, D. Singh, V. Dubey, N.S. Suryanarayana, Y. Parganiha, P. Jha, Review of the synthesis characterization, and properties of $LaAlO_3$ phosphors, Res. Chem. Intermed. (2013) 1–35, ISSN: 0922-6168.
[7] E. Celik, Y. Yamada, I. Hirabayashi, Y. Shiohara, Nb-doped $SrTiO_3$ buffer layers on $LaAlO_3$ substrates by metalorganic deposition for YBCO superconducting films, Mater. Sci. Eng.: B 110 (2004) 94–102.
[8] A.K. Kar, A. Dhar, S.K. Ray, B.K. Mathur, D. Bhattacharya, K.L. Chopra, Scanning tunneling microscopy and spectroscopy of $La_{0.67}Ca_{0.33}MnO_3$ thin films grown on $LaAlO_3$(100), Mater. Sci. Eng.: B 68 (1999) 10–15.
[9] C.R. Cho, Hetero-epitaxial growth and switching behaviors of PZT(53/47) films on $LaNiO_3$-deposited $LaAlO_3$ and $SrTiO_3$ substrates, Mater. Sci. Eng.: B 64 (1999) 113–117.
[10] V.H. Oliveira, N.M. Khaidukov, E.C. Silva, L.O. faria study of TL properties of $LaAlO_3$:Ce, Dy crystals for UV dosimetry, Radiat. Meas. 46 (10) (2011), 11731175.
[11] A.M. Hernández, J.Z. Medina, M.E. García, J.A. Nieto, T.R. Montalvo, Synthesis and thermoluminescence of $LaAlO_3$:Pr^{3+} to UVC radiation dosimetry, Appl. Radiat. Isot. 118 (2016) 12–17.
[12] N. Alves, W.B. Ferraz, L.O. Faria, Synthesis and investigation of the luminescent properties of carbon doped lanthanum aluminate ($LaAlO_3$) for application in radiation dosimetry, Radiat. Meas. 71 (2014) 90–94.
[13] H.F. Blum, Carcinogenesis by Ultraviolet Light, Princeton University Press, New Jersey, 1959.
[14] L.R. Koller, Ultraviolet Radiation, second ed., John Wiley & Sons New York, New York, USA, 1965.
[15] T. Rivera, C. Furetta, J. Azorín, C. Falcony, M. García, E. Martínez, Thermoluminescent properties of high sensitive ZrO_2-PTFE for UV radiation dosimetry, Mater. Sci. Forum 480–481 (2005) 373–380.
[16] L.E. Colyott, M.S. Akselrod, S.W.S. McKeever, An integrating ultraviolet-B dosemeter using photo transferred thermoluminescence from a-Al_2O_3:C, Radiat. Prot. Dosim. 72 (2) (1997) 87–94.
[17] M.S. Akselrod, V.S. Kortov, D.J. Kravetsky, V.I. Gotlib, Highly sensitive thermoluminescent anion-defective alpha-Al_2O_3:C single crystal detectors, Radiat. Prot. Dosim. 32 (1) (1990) 15–20.
[18] (b) X.B. Yang, H.J. Li, Q.Y. Bi, Y. Cheng, Q. Tang, J. Xu, Influence of carbon on the thermoluminescence and optically stimulated luminescence of Al_2O_3:C crystals, J. Appl. Phys. 104 (2008) 123112;
P.N. Scherrer, Zsigmondy's Kolloidchemie, Nachrichten der Göttinger Gesellschaft. 2 (1918) 98.
[19] J. Zhu, K.P. Muthe, R. Pandey, Stability and electronic properties of carbon in α-Al_2O_3, J. Phys. Chem. Solids 75 (2014) 379–383.
[20] A. Neumann, D. Walter, The thermal transformation from lanthanum hydroxide to lanthanum hydroxide oxide, Thermochim. Acta 445 (2006) 200–204.
[21] Peter Fleming, Richard A. Farrell, Justin D. Holmes, Michael A. Morrisw, The rapid formation of La(OH)3 from La2O3 powders on exposure to water vapor, J. Am. Ceram. Soc. 93 (2010) 1187–1194.
[22] C. Soliman, M.A. Husseinb, Lanthanum oxide as a new ultraviolet radiation dosimeter, Radiat. Effects Defects Solids: Incorp. Plasma Sci. Plasma Technol. 165 (1) (2010) 23–29.
[23] G. Kitis, G.M. Gomez-Ros, J.W.N. Tuyn, Thermoluminescence glow-curve deconvolution functions for first, second and general orders of kinetics, J. Phys. D: Appl. Phys. 31 (1998) 2636–2641.